The surprising magnetic topology of τ Sco: fossil remnant or dynamo output?[*]

J.-F. Donati[1]†, I.D. Howarth[2], M.M. Jardine[3], P. Petit[1], C. Catala[4],
J.D. Landstreet[5], J.-C. Bouret[6], E. Alecian[4], J.R. Barnes[3], T. Forveille[7],
F. Paletou[1] and N. Manset[7]

[1] *LATT, Observatoire Midi–Pyrénées, 14 Av. E. Belin, F–31400 Toulouse, France*
[2] *Department of Physics and Astronomy, University College London, Gower Street, London WC1E6BT, UK*
[3] *School of Physics and Astronomy, University of St Andrews, St Andrews, Scotland KY16 9SS, UK*
[4] *LESIA, CNRS–UMR 8109, Obs. de Paris, 5 Place Janssen, F–92195 Meudon Cedex, France*
[5] *Department of Physics and Astronomy, University of Western Ontario, London Ontario N6A3K7, Canada*
[6] *LAM, Observatoire de Marseille-Provence, Traverse du Siphon BP 8, F–13376 Marseille Cedex 12, France*
[7] *CFHT, 65-1238 Mamalahoa Hwy, Kamuela HI, 96743 USA*

ABSTRACT

We report the discovery of a medium-strength ($\sim$0.5 kG) magnetic field on the young, massive star τ Sco (B0.2 V), which becomes the third-hottest magnetic star known. Circularly polarized Zeeman signatures are clearly detected in observations collected mostly with the ESPaDOnS spectropolarimeter, recently installed on the 3.6-m Canada–France–Hawaii Telescope; temporal variability is also clearly established in the polarimetry, and can be unambiguously attributed to rotational modulation with a period close to 41 d. Archival UV spectra confirm that this modulation repeats over timescales of decades, and refine the rotation period to 41.033 ± 0.002 d.

Despite the slow rotation rate of τ Sco, we nonetheless succeed in reconstructing the large-scale structure of its magnetic topology. We find that the magnetic structure is unusually complex for a hot star, with significant power in spherical-harmonic modes of degree up to 5. The surface topology is dominated by a potential field, although a moderate toroidal component is probably present. We fail to detect *intrinsic* temporal variability of the magnetic structure over the 1.5-yr period of our spectropolarimetric observations (in agreement with the stable temporal variations of the UV spectra), and infer that any differential surface rotation must be very small.

The topology of the extended magnetic field that we derive from the photospheric magnetic maps is also more complex than a global dipole, and features in particular a significantly warped torus of closed magnetic loops encircling the star (tilted at about 90° to the rotation axis), with additional, smaller, networks of closed field lines. This topology appears to be consistent with the exceptional X-ray properties of τ Sco and also provides a natural explanation of the variability observed in wind-formed UV lines. Although we cannot completely rule out the possibility that the field is produced through dynamo processes of an exotic kind, we conclude that its magnetic field is most probably a fossil remnant from the star-formation stage.

Key words: stars: magnetic fields – stars: winds – stars: rotation – stars: early type – stars: individual: τ Sco – techniques: spectropolarimetry

1 INTRODUCTION

Magnetic fields in hot, high-mass stars of spectral types O and early B may have a drastic influence on the physics of the stellar interiors (e.g., Spruit 2002) and atmospheres (e.g., Babel & Montmerle 1997). As a consequence, they can also significantly modify these stars' long-term evolution, and in particular their rotational history (e.g., Maeder & Meynet 2003, 2004, 2005). However, quantifying these effects requires that we know the basic properties of such fields.

From a theoretical point of view, several quite different mechanisms have been proposed as potential means of generating large-scale magnetic fields in very hot stars. For example, such fields may be fossil remnants of the star-formation stage, either as relics of the field that pervaded the interstellar medium from which the star formed, or as leftovers from dynamo action in the convective Hayashi phase. This hypothesis was initially proposed for the lower-mass, chemically peculiar, magnetic Ap and Bp stars (e.g., Moss 2001) and has recently been rediscussed for the particular case of high-mass O and early-B stars by Ferrario & Wickramasinghe (2005, 2006); in this scenario, very hot magnetic stars are expected to be the progenitors of magnetic neutron stars.

A second possibility is that fields may be produced by continuing dynamo action; this option, initially suggested about two decades ago (e.g., Moss 1982), has not been closely examined until quite recently, but is now attracting increasing interest from theoreticians. A dynamo action could operate in the convective core (Charbonneau & MacGregor 2001; Brun et al. 2005), but the outer radiative envelope could also be involved in genuine dynamo processes, in a subsurface shear layer (Tout & Pringle 1995; Lignières et al. 1996) or even throughout the whole envelope (Spruit 2002; MacDonald & Mullan 2004; Mullan & MacDonald 2005; Maeder & Meynet 2005; Braithwaite 2006).

Unfortunately, all available theoretical options still suffer significant problems. Fossil-field theories have yet to demonstrate that sufficient magnetic flux can survive the accelerated decay and expulsion associated with Hayashi convection[1], while core-dynamo theories are still lacking detailed models linking the field produced in the core with that emerging at the surface (Moss 2001). Being based on a very new idea, radiative-zone dynamo theories are still in their infancy and need to establish their potential validity, by demonstrating that, in particular, stellar radiative zones are capable of sustaining differential rotation throughout their whole volume.

In addition to these issues, existing theories face a number of problems when compared to observations. At some point, all theories involve the coexistence of large-scale toroidal fields in stellar interiors and possibly even close to the surface (e.g., Braithwaite & Spruit 2004; Braithwaite & Nordlund 2006), which observations of magnetic Ap and Bp stars do not yet confirm (Moss 2001). More-

over, dynamo theories predict magnetic topologies that are expected to vary on short timescales and to depend strongly on stellar rotation rates, which again is not observed in intermediate-mass magnetic stars (Moss 2001). Last but not least, dynamos theories should in principle apply to most hot stars (as they do for most cool stars), making it hard to understand why only a small fraction of them (about 10% in the case of Ap/Bp stars) apparently hosts magnetic fields.

Indirect evidence for the presence of magnetic fields in high-mass stars is regularly reported in the literature, these being postulated as a potential explanation for many otherwise enigmatic phenomena, including unanticipated X-ray line profiles and high X-ray temperatures (e.g., Cohen et al. 1997; Robinson et al. 2002; Cohen et al. 2003; Smith et al. 2004). However, with *direct* detections of magnetic fields in only two O stars to date (Donati et al. 2002, 2006), together with less than a handful of early-B stars with masses larger than 10 $M_\odot$ (e.g., Donati et al. 2001; Neiner et al. 2003), very little is known reliably about magnetic strengths and topologies from a statistical point of view. One reason for this is that absorption lines of these stars are not only relatively few in number in the optical, but are also generally rather broad (due to rotation, or to some other type of as yet unknown macroscopic mechanism; e.g., Howarth et al. 1997), decreasing dramatically the size of the Zeeman signatures that their putative fields can induce.

In these respects, τ Sco (HR 6165, HD 149438, HIP 81266) appears as a very promising target for magnetic-field studies; thanks to its brightness and unusually narrow absorption lines (among the sharpest known for stars more massive than 10 $M_\odot$), τ Sco is an obvious candidate for accurate spectropolarimetric experiments. Moreover, its strong, hard X-ray emission (with $\log L_{\rm X}/L_{\rm Bol} \simeq -6.5$, Cohen et al. 1997) poses a severe challenge to the standard picture of O-star wind-shock models, leading some authors (e.g., Cohen et al. 2003) to speculate that it displays the presence of a magnetically confined wind, as proposed by Stahl et al. (1996) and Babel & Montmerle (1997), and as detected on the very young O star θ^1 Ori C (Donati et al. 2002; Gagné et al. 2005b,a). We therefore included τ Sco in a list of candidates for observation with ESPaDOnS, a high-efficiency spectropolarimeter installed in 2004/5 on the 3.6-m Canada–France–Hawaii Telescope (CFHT; Donati et al., 2006, in preparation).

In this paper, we first present our new spectropolarimetric observations and Zeeman detections obtained for τ Sco, and briefly summarize the UV spectra (Sec. 2). We then carry out a basic analysis of these data to establish the rotation period (Sec. 3), and review the fundamental stellar parameters in the light of our result (Sec. 4). We perform detailed modelling of the magnetic topology of τ Sco, by direct fitting to the observed Zeeman signatures (Sec. 5). Finally, we discuss the implications of our results for models of the X-ray emitting magnetosphere of τ Sco, as well for as theories of large-scale magnetic-field generation in high-mass stars (Secs. 6 and 7).

(TF); fpaletou@ast.obs-mip.fr (FP); manset@cfht.hawaii.edu (NM)

[1] This difficulty may not be as problematical as it first seemed, as discussed in Moss (2003), and should not concern stars with masses larger than 10 $M_\odot$.

Table 1. Journal of spectropolarimetric observations. Columns 1–6 list the UT date & time, heliocentric Julian date (all at mid-exposure), observing site, exposure time, and peak signal to noise ratio (per 2.6 km s^{-1} velocity bin) of each observation. Columns 7 and 8 list the rms noise level (per 1.8 km s^{-1} velocity bin, relative to the unpolarized continuum level I_c) in the circular-polarization profile produced by Least-Squares Deconvolution (see Sec. 2) and the estimated longitudinal field B_ℓ (with corresponding 1σ error bars). The rotational cycle E from the ephemeris of eqn. 1 is given in column 9.

UT Date	(h:m:s)	HJD (2,453,000+)	Obs	$t_{\exp}$ (s)	S/N	$\sigma_{\rm LSD}$ ($10^{-4}I_c$)	B_ℓ (G)	Cycle
2004 Sep. 04	05:58:31	252.7475	CFHT	4×30	1440	0.70	-24.4 ± 3.3	1.456
2004 Sep. 04	06:23:17	252.7647		4×30	1280	0.75	-18.3 ± 3.4	1.457
2004 Sep. 25	05:03:15	273.7075	CFHT	4×30	1060	0.96	$+36.2 \pm 4.5$	1.967
2004 Sep. 25	05:10:24	273.7124		2×60	1100	0.92	$+47.5 \pm 4.3$	1.967
2004 Sep. 26	08:51:15	274.8689	AAT	4×120	890	1.03	$+64.0 \pm 4.2$	1.995
2004 Sep. 27	08:52:49	275.8700		4×120	860	1.10	$+78.4 \pm 4.5$	2.020
2004 Sep. 28	08:58:25	276.8739		4×120	670	1.36	$+80.5 \pm 5.6$	2.044
2005 May 23	09:14:25	513.8903	CFHT	4×300	1700	0.63	-47.9 ± 3.0	7.820
2005 May 24	08:32:52	514.8614		4×60	900	1.17	-50.3 ± 5.6	7.844
2005 May 25	08:41:35	515.8675		4×60	880	1.19	-41.4 ± 5.5	7.868
2005 June 19	07:19:19	540.8096	CFHT	4×120	1200	0.85	-19.2 ± 4.3	8.476
2005 June 20	06:44:15	541.7852		4×120	1550	0.66	-20.2 ± 3.3	8.500
2005 June 21	06:51:16	542.7900		4×120	1650	0.62	-19.8 ± 2.9	8.525
2005 June 22	08:42:17	543.8671		4×120	1440	0.71	-12.8 ± 3.6	8.551
2005 June 23	06:07:24	544.7595		4×120	1670	0.61	-5.9 ± 3.1	8.572
2005 June 24	06:22:32	545.7699		4×120	1710	0.60	$+1.3 \pm 3.1$	8.597
2005 June 25	06:05:50	546.7583		4×120	1570	0.68	$+4.7 \pm 3.4$	8.621
2005 June 26	06:00:31	547.7545		4×120	1590	0.66	$+0.9 \pm 3.3$	8.646
2005 June 26	11:02:47	547.9644		4×120	1370	0.82	-5.1 ± 4.2	8.651
2005 Aug. 19	05:20:15	601.7224	CFHT	4×30	1250	0.77	$+44.5 \pm 3.7$	9.961
2005 Aug. 21	05:21:43	603.7232		4×30	1200	0.81	$+80.3 \pm 4.0$	10.010
2005 Aug. 23	05:11:45	605.7161		4×30	1150	0.85	$+87.8 \pm 4.2$	10.058
2005 Sep. 19	05:03:10	632.7079	CFHT	4×30	1180	0.83	-21.8 ± 3.7	10.716
2005 Sep. 20	05:01:56	633.7070		4×30	1280	0.76	-28.9 ± 3.6	10.740
2005 Sep. 24	04:55:44	637.7023		2×50	680	1.48	-45.9 ± 6.8	10.838
2005 Sep. 25	04:48:19	638.6971		4×30	1200	0.83	-51.9 ± 5.3	10.862
2005 Sep. 25	05:01:33	638.7063		4×30	1120	0.89	-43.4 ± 4.2	10.862
2006 Feb. 07	15:03:44	774.1269	CFHT	4×30	1090	0.88	$+44.9 \pm 4.1$	14.162
2006 Feb. 08	16:22:33	775.1817		4×30	910	1.04	$+44.3 \pm 4.8$	14.188
2006 Feb. 09	16:16:56	776.1779		4×30	620	1.58	$+38.9 \pm 7.0$	14.212
2006 Feb. 10	16:33:25	777.1895		4×30	1250	0.76	$+32.8 \pm 3.4$	14.237
2006 Feb. 11	16:18:20	778.1791		4×30	1020	0.94	$+25.8 \pm 4.2$	14.261
2006 Feb. 13	16:15:23	780.1772		4×30	490	2.06	$+35.4 \pm 9.4$	14.310
2006 Feb. 14	16:23:12	781.1827		4×30	840	1.13	$+0.6 \pm 5.6$	14.334
2006 Feb. 15	14:07:12	782.0884		4×30	1060	0.92	$+8.0 \pm 4.5$	14.357

2   OBSERVATIONS

2.1   Optical spectropolarimetry

Spectropolarimetric observations of τ Sco were collected with ESPaDOnS from 2004 Sep. to 2006 Feb., during the first engineering runs (in 2004, when the field was first detected) and subsequently for scheduled ESPaDOnS programmes. The ESPaDOnS spectra span the entire optical domain (from 370 to 1,000 nm) at a resolving power of about 65,000. In total, 32 circular-polarization sequences were collected, most of them consisting of 4 individual subexposures taken in different polarimeter configurations (in two cases, the sequence was interrupted after the second exposure due to a technical problem with the instrument control). The extraction procedure is described in Donati et al. (1997, see

Donati et al., 2006, in prep., for further details) and was carried out with Libre ESpRIT, a fully automatic reduction package/pipeline installed at CFHT for optimal extraction of ESPaDOnS spectra. The peak signal-to-noise ratios per 2.6 km s^{-1} velocity bin range from 490 to 1710, depending mostly on weather conditions and exposure time (see Table 1)[2].

Three additional circular-polarization spectra were obtained at the 3.9-m Anglo-Australian Telescope (AAT) in late Sep. 2004, using a visitor-instrument Cassegrain po-

---

[2] Note that the instrument suffered a 1.3-mag loss in throughput compared to the optimal performance from early March to late June 2005, due to severe damage to the external jacket of optical fibres linking the polarimeter with the spectrograph (now fixed).
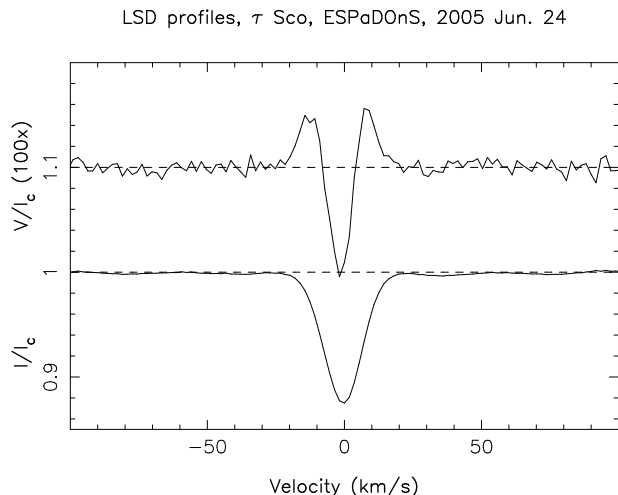
LSD profiles, τ Sco, ESPaDOnS, 2005 Jun. 24

Figure 1. LSD unpolarized and circularly polarized profiles of τ Sco (bottom, top curves respectively), as observed on 2005 June 24. The mean polarization profile is expanded by a factor of 100 and shifted upwards by 1.10 for display purposes.

larimeter, fibre linked to the UCL echelle spectrograph (UCLES), in a setup very similar to that described by Donati et al. (2003). The AAT spectra, processed with the same reduction package as used for the CFHT data, cover 430–670 nm at a resolving power of 65,000. The peak signal-to-noise ratios per 2.6 $km\,s^{-1}$ velocity bin range from 670 to 890, depending on the weather (see Table 1).

Both instruments use Fresnel rhombs (rather than crystalline plates) as retarders, with the result that spectropolarimetric ripples (e.g., Aitken & Hough 2001; Semel 2003) are decreased down to a level below detectability. An example of this improvement compared to previous otherwise similar instruments (such as the MuSiCoS spectropolarimeter; Donati et al. 1999) is illustrated by Wade et al. (2005) and Wade et al. (2006) in the particular case of hot-star observations.

In order to gain a multiplexing advantage by combining results from different lines in the spectra, Least-Squares Deconvolution (LSD; Donati et al. 1997) was applied to all observations. The line list required for LSD was computed from an Atlas9 LTE model atmosphere (Kurucz 1993) at $T_{eff} = 30,000$ K, $\log g = 4.5$, roughly matching τ Sco's parameters. We utilized only moderately strong lines (those with synthetic profiles having line-to-continuum core depressions larger than 10% prior to all non-thermal broadening mechanisms, but omitting the very strongest, broadest features, such as Balmer and He lines, whose Zeeman signature is strongly smeared out compared to those of narrow lines) – some 500 spectral features altogether, with about half corresponding to oxygen lines and most others coming from N, Si, C and Fe. The average noise levels in the resulting LSD signatures range 0.6–2.1×10^{-4} for ESPaDOnS spectra and 1.0–1.4×10^{-4} for the AAT data (per 1.8-$km\,s^{-1}$ velocity bin, relative to the unpolarized continuum level I_c; see Table 1). Significant Zeeman signatures are clearly detected in all the spectra, with a full amplitudes of about 0.2%, demonstrating that a magnetic field is securely detected for τ Sco; an illustrative example is shown in Fig. 1.

The Zeeman signatures detected are variable with time[3] and correspond to projected longitudinal fields (computed from the first-order moment of the Stokes V LSD profile; Donati et al. 1997) ranging from -50 to $+90$ G (see Table 1). Our results are compatible with the earlier findings of Landstreet (1982) that longitudinal fields of normal upper-main-sequence stars in general, and of τ Sco in particular (for which Landstreet 1982 report two estimates), are less than 100 G on average.

2.2 UV spectroscopy

We augmented the new spectropolarimetric data set with archival UV spectra obtained with the International Ultraviolet Explorer satellite (IUE; Boggess et al. 1978). The IUE archive contains 107 high-resolution spectra of τ Sco, covering the wavelength range 115–195 nm, sampled at 0.01-nm intervals with a resolution of about 10^4 and S/N $\simeq$ 20. We examined spectra obtained from the MAST IUE archive at the Space Telescope Science Institute, reduced using NEWSIPS pipeline software (Nichols & Linsky 1996, the 'MXHI' product). IUE spectra were each acquired through one of two focal-plane apertures, designated 'small' and 'large'; we found indications of data-processing errors in a number of small-aperture spectra, which also generally have poorer signal and S/N than the large-aperture data (typically, the small aperture transmitted only ~half the incident radiation). We therefore present results based on only the 72 large-aperture spectra in the archive; incorporating the small-aperture data introduces no material changes to the conclusions.

3 THE ROTATION PERIOD OF τ SCO

3.1 Zeeman spectroscopy

Time variability of the projected longitudinal field is a potentially powerful tool for estimating stellar rotation periods, which often cannot be measured by other means. Specifically, temporal fluctuations of the line-of-sight component of the field in hot stars may be attributed to a magnetic topology that is not axisymmetric about the rotation axis, thus showing different configurations to the observer as the star rotates. Searching for timescales on which the longitudinal field repeats identically from one cycle to the next has been very successful in estimating rotation periods of Ap and Bp stars (e.g., Borra & Landstreet 1980).

Of course, the longitudinal-field values contain far less information about the field topology than the Zeeman signatures themselves. The Stokes V LSD profile shown in Fig. 1 provides a clear demonstration of this point; while the Zeeman signature strongly indicates a field detection (at a level of about 27σ), the corresponding longitudinal field is 1.3 ± 3.1 G and is therefore inconclusive by itself. Nonetheless, longitudinal-field values are convenient summary statistics in several respects, and in particular can provide useful

---

[3] The LSD I profiles are also variable in strength. The level of this variability is, however, small (about 0.3% rms of the continuum level, equivalent to ~3% of the central line depth), affecting mainly the line width. We return to this point in Sec. 4.

rough estimates of the average magnetic flux over the stellar surface.

As an initial step in modelling the longitudinal-field variations of τ Sco, we compared a double sine-wave fit to the data, with the two periods held in the ratio 2:1 (motivated by what we expect from a simple, rotationally modulated, linear combination of dipole plus quadrupole fields). For a range of assumed values for the longer (i.e., rotational) period, the amplitudes and phases of both waves were optimized to obtain the best fit to the longitudinal-field measurements, using a standard least-squares minimization process, with the reduced-χ^2 value, χ^2_ν, evaluated as the statistic of merit for the fit quality. Fig. 2 (upper panel) shows the results of this exercise, and indicates a strong minimum in χ^2_ν at $P_{\rm rot} = 41.08 \pm 0.07$ d (1σ uncertainty).

However, the double sine-wave model evidently provides no more than a rough fit to the data, with a minimum χ^2_ν as large as ~9. This, in turn, indicates that the field must be significantly more complex than a tilted dipole plus quadrupole combination, and must contain higher-order, multipole components.[4] Clearly, more-detailed modelling of the Zeeman signatures is necessary in order to obtain an adequate description of the magnetic topology of τ Sco; we describe such modelling in Sec. 5.

The mis-match between the simple model and the data means that the 41-d signal is no more than a provisional estimate of the rotation period. More accurate and precise values may be obtained both from modelling the Zeeman signatures directly (Sec. 5), and from a time-series analysis of the IUE data (Sec. 3.2).

3.2 UV line-profile variability

Direct measurement of magnetic fields in hot stars (e.g.; Donati et al. 2001, 2002; Neiner et al. 2003; Donati et al. 2006) has often been presaged by the detection of strictly periodic UV line-profile variability, with the inference of a magnetic field by analogy with He peculiar stars (e.g.; Stahl et al. 1996; Neiner et al. 2003; Walborn et al. 2004). A search for variability in the IUE spectra of τ Sco (known to exhibit abnormally strong UV P-Cygni lines; Walborn & Panek 1984) is therefore a natural follow-up to our detection of rotationally modulated Zeeman signatures in the spectropolarimetric data.

We are fortunate that τ Sco was adopted as a photometric calibration star by the IUE Project, and that as a consequence the temporal sampling of the UV spectra is rather well suited to investigating the rotational timescale identified in the Zeeman spectroscopy: the large-aperture spectra span 16.6 yr (1979 Feb – 1995 Sept, median date 1988 Aug) at a median sampling rate of 50.7 d (range 0.7 hr – 417 d).

We analyzed the rectified IUE spectra using the implementation of the CLEAN algorithm described by

---

[4] The rotational modulation of the longitudinal field is very reminiscent of what is observed on the helium-strong star HD 37776 (Thompson & Landstreet 1985), apart from the fact that the field of HD 37776 is stronger than that of τ Sco by more than an order of magnitude.
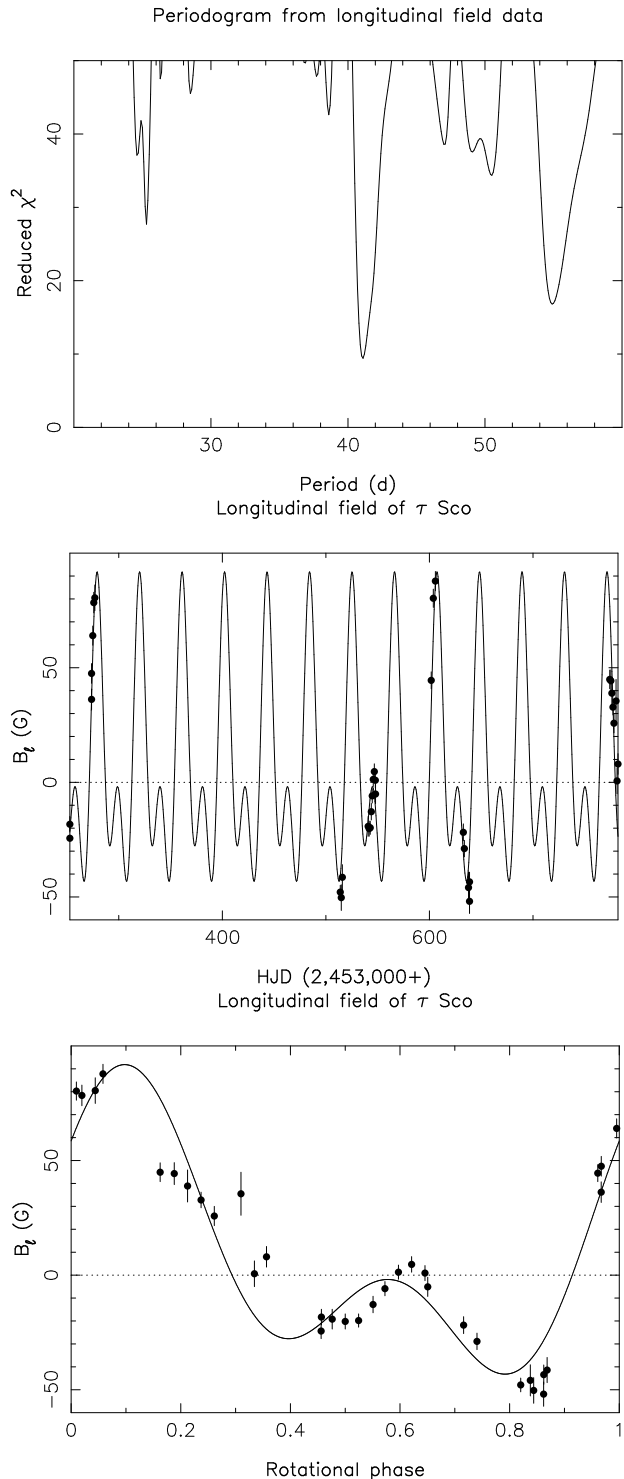

Figure 2. Periodogram resulting from a double sine-wave fit to the longitudinal-field data of τ Sco. *Top panel:* χ^2_ν as a function of the period of the main sine wave. A clear minimum is obtained for a period of about 41 d. *Middle panel:* Temporal fluctuations of the longitudinal field of τ Sco (full dots, with 1σ error bars) along with the model fit (full line) for the adopted period of 41.033 d, as a function of heliocentric Julian date (HJD). *Bottom panel:* As for the middle panel, but as a function of rotation phase, computed using the ephemeris of eqn. 1.
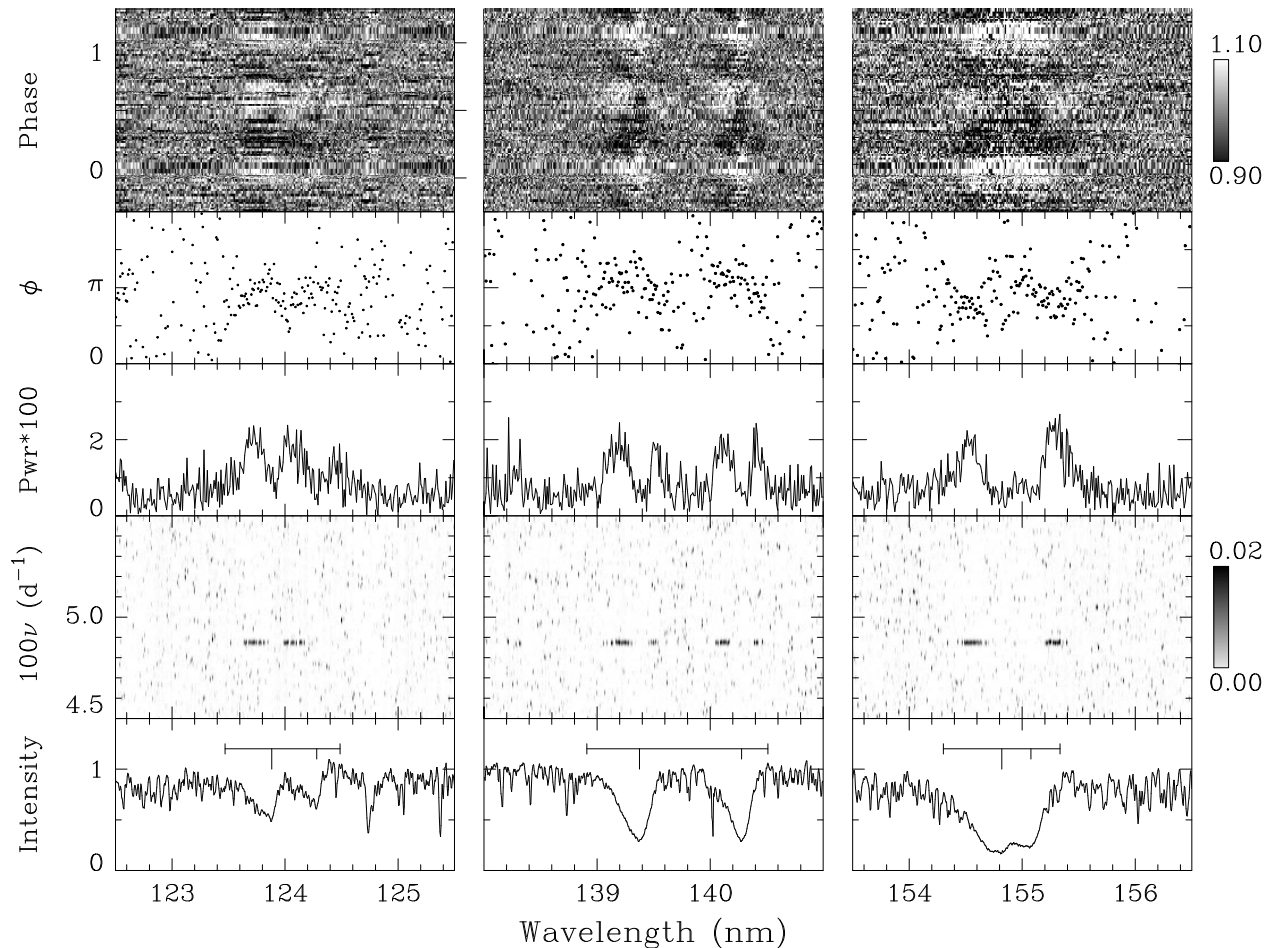
Figure 3. Time-series analysis of IUE spectra of τ Sco. The bottom panel shows the mean spectrum for (left to right) the N V, Si IV, and C IV resonance doublets; in each case, vertical tickmarks indicate the rest wavelengths, while the horizontal bar extends from 1000 km s^{-1} bluewards of the short-wavelength component to +500 km s^{-1} redwards of the long-wavelength component. The next panel up shows part of the 2D CLEANed periodogram, showing evidence for a periodic signal at $\nu = 0.049$ d^{-1} in the wind-formed lines (see Fig. 4), while the next two panels show the fourier power and phase, respectively, at that frequency. The top panel shows the residuals about the mean of the rectified spectra phased according to the ephemeris of eqn. 1.
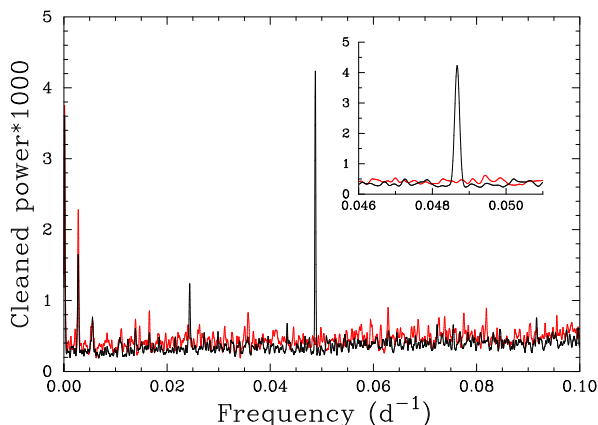

Figure 4. Mean power spectrum for regions extending 1000 km s^{-1} bluewards of the short-wavelength component to +500 km s^{-1} redwards of the long-wavelength component for the N V 124 nm, Si IV 140 nm, and C IV 155 nm resonance doublets (black line), and for equivalent regions 2 nm longwards (red line).

Roberts et al. (1987); some results of this analysis are presented in Fig. 3. There is a strong signal at $\nu = 0.049$ d^{-1} ($P = 20.5$ d) in the main features formed in the stellar wind (the N V 124 nm, Si IV 140 nm, and C IV 155 nm resonance lines, but also Si III 120.6 nm). To examine this in greater detail, we constructed the mean power spectrum for wavelengths from 1000 km s^{-1} bluewards of the short-wavelength component to 500 km s^{-1} redwards of the long-wavelength component for each of the three resonance doublets, together with a comparison spectrum from equivalent regions 2 nm longwards of each feature; results are shown in Fig. 4.

In addition to the main signal, there is a weak secondary signal at $\nu = 0.024$ d^{-1} (Fig. 4), corresponding to a period of about 41 d.[5] Since a period of 20.5 d is completely excluded by the Zeeman measurements (Sec. 3.1), we in-

---

[5] There are also signals, in both the main and reference datasets, at $P = 0.5$ yr and 1 yr. These are presumed to be non-astrophysical (and are most probably the result of varying background levels).

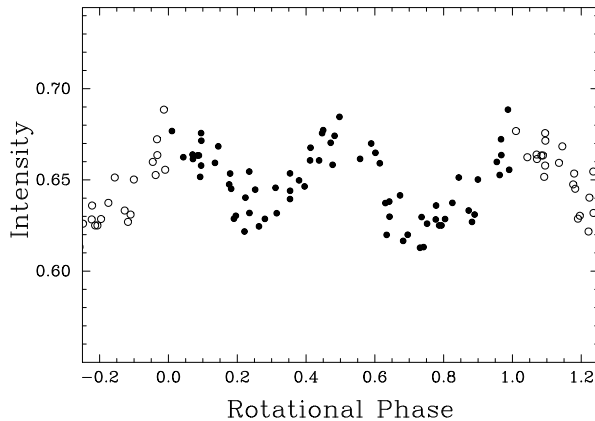**Figure 5.** Mean residual intensity for regions from $1000 \ \mathrm{km\,s^{-1}}$ bluewards of the short-wavelength component to $+500 \ \mathrm{km\,s^{-1}}$ redwards of the long-wavelength component for each of the N V 124 nm, Si IV 140 nm, and C IV 155 nm resonance doublets, as a function of rotational phase. Phases are computed according to the ephemeris of eqn. 1.

terpret our findings as indicating a slightly non-sinusoidal double wave with $P_{\mathrm{rot}} = 41.03$ d. To refine this period we average results from the 75 0.1-Å wavelength bins in the $-1000/+500 \ \mathrm{km\,s^{-1}}$ test ranges for which the peak of the power spectrum is safely identifiable with the $\nu = 0.049 \ \mathrm{d^{-1}}$ signal; half the mean peak frequency for those samples corresponds to $P_{\mathrm{rot}} = 41.033 \pm 0.002$ d (s.e.).

As an alternative characterization of the data, fitting a gaussian to the peak of the mean power spectrum yields $P\mathrm{rot} = 41.034$ d, and a full-width at half-maximum (FWHM) of 0.36 d. To obtain a second, reasonably conservative, estimate of the uncertainty on the period, we may assume that the signal does not go out of phase by more than $0.125 P_{\mathrm{rot}}$ (i.e., 0.25 of the 20.5-d half-wave period) in each of the contributing wavelengths, giving $P = 41.0340 \pm 0.0040$ d (s.e.).

We emphasize that the data are fully consistent with a strictly periodic signal; the IUE data, spanning almost 17 yr, show no evidence for any non-periodic component insofar as the width of the periodogram peak is entirely accounted for by the finite number of cycles in the dataset ($N = 148$). Moreover, the same period is recovered, to high accuracy, in completely independent datasets separated by a quarter-century (viz., the IUE and Zeeman spectroscopy; more-detailed modelling of the Zeeman data, reported in Sec. 5, yields $P_{\mathrm{rot}} = 41.02 \pm 0.03$ d). Furthermore, the precision of the adopted rotation period is high enough to ensure that the relative phasing between the archival IUE spectra and our new spectropolarimetric data is better than 1%.

On the basis of these results we therefore adopt

$$T_0 = \mathrm{HJD} \ 2,453,193.0 + 41.033(\pm 0.002)E \qquad (1)$$

as our rotational ephemeris, where phase zero is arbitrarily chosen for convenience as a date just prior to the acquisition of the first Zeeman data. The rotational modulation of the mean residual intensity over the N V, Si IV and C IV UV resonance doublets with this ephemeris is shown in Fig. 5; significant absorption episodes are observed to occur in all 3 spectral features around phase 0.3 and 0.8.

4 ROTATIONAL PROPERTIES

From our analysis, τ Sco is the second-slowest rotator so far known among high-mass stars (cp. HD 191612, whose rotation period is suggested to be 538 d; Donati et al. 2006). In order to be able to refine our modelling of its magnetic topology, we first summarize what we know about its physical parameters, and examine how these tie in with the rotation period we derive.

From detailed spectroscopic studies by Kilian (1992), Mokiem et al. (2005) and Simon-Diaz et al. (2006), we know that τ Sco is a young star, with an age of a few Myr[6], a mass of $\sim 15 \ \mathrm{M_\odot}$, a temperature of $31,500 \pm 500$ K, and a radius of $5.2 \pm 0.5 \ \mathrm{R_\odot}$.[7] The radius and rotation period imply an equatorial rotation velocity, v_{e}, of only $6.4 \pm 0.6 \ \mathrm{km\,s^{-1}}$, and thus a line-of-sight projected rotation velocity, $v_{\mathrm{e}} \sin(i)$, which is even less (where i is the inclination of the rotation axis to the line of sight). This $v_{\mathrm{e}} \sin(i)$ limit is significantly lower than the estimate given by Kilian (1992) from line-profile modelling ($19 \ \mathrm{km\,s^{-1}}$), but is similar the value (of $5 \ \mathrm{km\,s^{-1}}$) reported by both Smith & Karp (1978) and Mokiem et al. (2005), and is consistent with the upper limit given by Simon-Diaz et al. (2006, $13 \ \mathrm{km\,s^{-1}}$).

We performed our own simple modelling of the LSD Stokes I profile, to get an estimate of how much (and what type of) broadening is required in addition to a pure rotational broadening in order to obtain a reasonable fit to the data. We find that gaussian broadening with an average FWHM of $13.5 \ \mathrm{km\,s^{-1}}$ gives a nice match to the mean LSD profile (after allowance for a gaussian instrumental broadening, with a FWHM of $5 \ \mathrm{km\,s^{-1}}$). This corresponds to a turbulent velocity of about $8 \ \mathrm{km\,s^{-1}}$, a value similar to estimates given by Mokiem et al. (2005) and Simon-Diaz et al. (2006, 10.8 and $8.7 \ \mathrm{km\,s^{-1}}$, respectively). This broadening is larger than the thermal broadening expected for most lines used in the LSD process (about $5 \ \mathrm{km\,s^{-1}}$ in average, ranging from 3 to $6 \ \mathrm{km\,s^{-1}}$, depending on the atom), and the similar widths found for lines from different atoms confirm that the main origin is non-thermal.

As already mentioned in Sec. 2, we observe that the Stokes I LSD profiles of τ Sco are slightly variable with time, and that this temporal variation can also be attributed as modulation with the 41 d rotation period derived at Sec. 3 (see Fig. 6). This modulation consists mainly of a small $\sim 10\%$, phase-locked variation of the line width, with the average photospheric profile being slightly narrower around phase 0.5. We suspect that this indicates that the atmospheric turbulence evinced by the line broadening is induced at the base of the wind, and is not constant over the surface of τ Sco, reflecting, perhaps, the spatial distribution of field strengths and orientations; another possibility is that the density at the base of the wind is not constant over the surface of the star (again, as a potential result of the magnetic

---

[6] Although τ Sco is quoted to be younger than 1 Myr by Kilian (1992), its membership in the Sco OB2 association (de Zeeuw et al. 1999) suggests that τ Sco, as the most massive star in the group, is roughly as old as the group itself – i.e., nearly 5 Myr.

[7] Significantly larger radii are cited in the literature, e.g. by Howk et al. 2000, but they are not consistent with the well-established Hipparcos parallax.
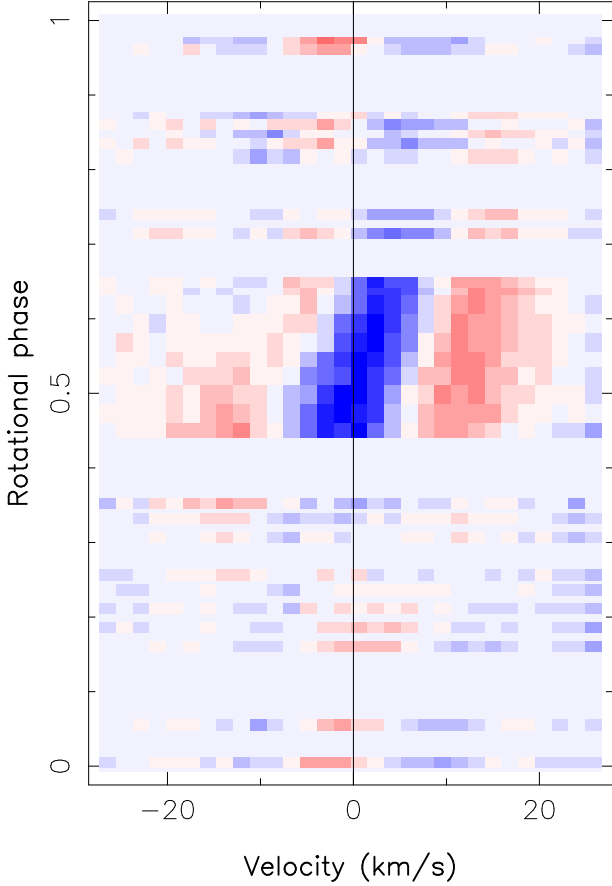
Figure 6. Dynamic LSD Stokes I spectrum of τ Sco, demonstrating that the average unpolarised line is also modulated with the detected rotation period of 41 d (see Sec. 3). A simple synthetic profile (featuring gaussian turbulence broadening with a FWHM of 13.5 km s^{-1} and $v_e \sin(i) = 6$ km s^{-1}, see text) was removed from all profiles to emphasize variability. A clear signal, centred at phase 0.5, crosses the line profile and indicates that the average photospheric line of τ Sco gets slightly narrower (by about 10%) around phase 0.5. Blue and red respectively correspond to line absorption/emission features with an amplitude of $\pm 0.4\%$ of the continuum intensity (i.e. $\pm 3\%$ of the central line depth).

field), causing the observer to see to different atmospheric depths (and thus different turbulent broadenings) at different rotational phases. We also find that a slightly better fit to the Stokes V signatures is obtained when assuming a local line profile width about 10% narrower than that derived from LSD Stokes I profiles; we speculate that Zeeman signatures are formed at atmospheric depths slightly different from the unpolarised spectral lines, i.e. in a layer where turbulent broadening is weaker.

From the observed variability of the longitudinal field, which in particular shows a steep gradient as well as a sign switch in as little as 10% of the rotational cycle (between phase 0.85 and 0.95; see Fig. 2, bottom panel), we conclude that it is unlikely that τ Sco is seen near-pole-on; modelling of the Zeeman signatures (Sec. 5) reveals that significantly better fits to the data are obtained with $v_e \sin(i) = 6$ km s^{-1} than with values ≤ 5 km s^{-1}. This implies that i is large, probably in the range $60°$–$90°$. Since there is only a low probability that the star is seen exactly equator on, we assume $i = 70°$ (and $v_e \sin(i) = 6$ km s^{-1}) in the following analysis. Very similar results are obtained with values of i ranging from $60°$ to $90°$.

Finally, we note that the radial velocity of τ Sco has remained remarkably stable during the whole length of our run, at -0.6 ± 0.1 km s^{-1}. This confirms earlier conclusions by Stickland & Lloyd (1995) that there is no reason to suppose that τ Sco a member of a binary system.

5 MODELLING THE SURFACE MAGNETIC TOPOLOGY OF τ SCO

5.1 Methodology

To reconstruct the surface magnetic topology of τ Sco from the set of observed Zeeman signatures, we use our magnetic-imaging code (Brown et al. 1991; Donati & Brown 1997) in its most recent implementation (Donati 2001). While still based on maximum-entropy image reconstruction, this latest version reconstructs the field topology as a spherical-harmonic decomposition, rather than as a series of independent magnetic-image pixels as before. One obvious advantage of this method is that we can impose *a priori* constraints on the field topology – e.g., that the field is purely potential, or purely toroidal, or a combination of both. Another important advantage of this formalism is that both simple and complex magnetic topologies can easily be reconstructed (Donati 2001), whereas the original method failed at reconstructing simple magnetic geometries (such as dipoles; Brown et al. 1991).

To effect this approach, we describe the field as the sum of a potential and a toroidal component, each expressed as a spherical-harmonic expansion. In a formalism similar to that of Jardine et al. (1999), the field components can be written as:

$$B_r(\theta,\phi) = -\sum_{\ell,m} \alpha_{\ell,m} Y_{\ell,m}(\theta,\phi) \quad (2)$$

$$B_\theta(\theta,\phi) = -\sum_{\ell,m} \left(\beta_{\ell,m} Z_{\ell,m}(\theta,\phi) + \gamma_{\ell,m} X_{\ell,m}(\theta,\phi) \right) \quad (3)$$

$$B_\phi(\theta,\phi) = -\sum_{\ell,m} \left(\beta_{\ell,m} X_{\ell,m}(\theta,\phi) - \gamma_{\ell,m} Z_{\ell,m}(\theta,\phi) \right), \quad (4)$$

where

$$Y_{\ell,m}(\theta,\phi) = c_{\ell,m} P_{\ell,m}(\theta)\, e^{im\phi} \quad (5)$$

$$Z_{\ell,m}(\theta,\phi) = \frac{c_{\ell,m}}{\ell+1} \frac{\partial P_{\ell,m}(\theta)}{\partial\theta}\, e^{im\phi} \quad (6)$$

$$X_{\ell,m}(\theta,\phi) = \frac{c_{\ell,m}}{\ell+1} \frac{P_{\ell,m}(\theta)}{\sin\theta}\, im\, e^{im\phi} \quad (7)$$

$$c_{\ell,m} = \sqrt{\frac{2\ell+1}{4\pi} \frac{(\ell-m)!}{(\ell+m)!}}, \quad (8)$$

with ℓ and m denoting the order and degree of the spherical-harmonic mode $Y_{\ell,m}(\theta,\phi)$ (θ and ϕ being the colatitude and longitude at the surface of the star), and $P_{\ell,m}(\theta)$ the associated Legendre polynomial. For a given set of the complex coefficients $\alpha_{\ell,m}$, $\beta_{\ell,m}$ and $\gamma_{\ell,m}$ (where $\alpha_{\ell,m}$ characterises the radial field component, $\beta_{\ell,m}$ the azimuthal and meridional components of the potential field term, and $\gamma_{\ell,m}$ the azimuthal and meridional components of the toroidal field term), one can produce the associated magnetic image at

the surface of the star, and thus derive the corresponding Stokes V dataset. We carry out the inverse problem, aimed at reconstructing a set of complex coefficients from an automated, iterative fit to the observed circular-polarization LSD profiles. Principles of maximum-entropy image reconstruction are applied to the set of complex coefficients, rather than on the image pixels. This is similar to what is presented by Hussain et al. (2001), except that we generalize the problem to fields that are non-potential and feature a significant toroidal component. Fitting a pure potential field to the data is equivalent to fitting $\alpha_{\ell,m}$ and $\beta_{\ell,m}$ alone (setting all $\gamma_{\ell,m}$ to zero); using all three sets of coefficients in the fitting procedure produces a more general magnetic topology, with a non-zero toroidal field. Trying both approaches is a straightforward way of investigating whether or not the magnetic field at the surface of τ Sco is potential in nature.

For a spectral resolution of 5 km s^{-1}, a microturbulent velocity of 7.5 km s^{-1}, and a projected equatorial velocity $v_e \sin(i)$ of 6 km s^{-1}, the number of resolved equatorial elements around the star is about 5, implying that we need about 10 equatorial elements to reproduce the observations with adequate surface sampling. Truncating the spherical-harmonic expansion of the magnetic-field components to terms with $\ell \leq 10$ is therefore sufficient in the case of τ Sco, and should introduce negligible degradation in the spatial resolution of our reconstructed images. In practice, we used $\ell \leq 12$ and found that, as expected, no improvement in the quality of the fit to the data was obtained when adding higher-order terms. This corresponds to mapping a total of 90 modes at the surface of the star, implying a total of 360 image parameters in the case of a potential field, and 540 in the case of a potential- plus toroidal-field configuration.

We first carried out a series of magnetic reconstructions for a wide range of values of the rotation period (without constraining the field to a specific type of configuration). The minimum χ_ν^2 is obtained at $P_{\rm rot} = 41.02 \pm 0.03$ d (1σ uncertainty). This estimate of $P_{\rm rot}$ is a refinement of that derived in Sec. 3.1, because of the more complete physical model; it is fully compatible with the adopted, more precise period derived independently from the IUE data (eqn. 1; Sec. 3.2).

The best-fit model of the Zeeman signatures is shown in Fig. 7, from which it is obvious that the greater part of the observed profile information is satisfactorily reproduced. Nonetheless, the minimum χ_ν^2 is as large as 1.5, indicating that discrepancies between the model and observations still exist. The origin of these (small) discrepancies is not yet clear, but may result from the simple isotropic local line-profile model we use to compute the synthetic Stokes V profiles (Sec. 4). We note that the fit to the data is much worse if we force the magnetic topology to be very simple, e.g., similar to that found in most magnetic chemically peculiar stars to date. For instance, when truncating the spherical harmonics expansion to $\ell \leq 1$ (equivalent to fitting the data with a tilted magnetic dipole model), the minimum achievable χ_ν^2 is 15; with $\ell \leq 2$ (roughly equivalent to adding up a magnetic quadrupole component to the model), the fit quality is still very rough ($\chi_\nu^2 \simeq 8$). The detected Stokes V profiles (and in particular the observed rotational modulation) definitely indicate that the magnetic-field topology of τ Sco is much more complex than usual (by massive star standards).

5.2 Results

The magnetic topology we reconstruct by assuming that the field includes both a potential field and a toroidal field component is shown in Fig. 8. The corresponding χ_ν^2 is 1.5. If we instead assume that the field is purely potential, the optimal fit we obtain yields $\chi_\nu^2 = 1.8$, indicating a slightly poorer fit; while the inferred topology is broadly similar to that shown in Fig. 8, the contrast and information content is significantly higher than in the previous case. We can thus say that, at given image information content, the potential- plus toroidal-field configuration provides a significantly better fit than the pure potential-field configuration (with respective χ_ν^2 values of 1.5 and 1.8), indicating that the first option appears significantly more likely than the latter.

The contributions of potential and toroidal terms to the azimuthal and meridional field components are shown separately in Fig. 9 (the toroidal term does not contribute to the radial field component). We therefore conclude that the surface magnetic topology of τ Sco is mainly potential, but apparently also includes a toroidal field component. We find that the potential field component includes about 70% of the overall reconstructed magnetic energy, and thus clearly dominates over the toroidal field component. In particular, we note that, compared to the potential component, this toroidal component is much weaker in τ Sco than in most cool magnetic stars observed to date, where the toroidal component largely exceeded the poloidal one (e.g., Donati et al. 2003). Moreover, we find that this toroidal component is not primarily axisymmetric (at least about the rotation axis), featuring for instance two sign switches (at phases 0.52 and 0.18) at equatorial latitudes (see Fig. 9, top right panel).

The results further emphasize that the reconstructed magnetic field is far more complex than a simple dipole; for example, the polarity of the radial field component switches sign six times along the equator (instead of just twice as expected for a tilted dipole). A more quantitative way of considering the complexity of the field is to examine the relative strengths of the reconstructed spherical-harmonic coefficients $\alpha_{\ell,m}$, $\beta_{\ell,m}$ and $\gamma_{\ell,m}$ (see Fig. 10). Even though the modes corresponding to a tilted dipole are excited ($\ell = 1$ and $m = 0 - 1$), a large number of other modes carry significant power (especially sectoral modes); the $\ell = m = 4$ mode is among the strongest, and its signature can be readily seen from the magnetic images of Fig. 8. Unsurprisingly, modes with $\ell > 6$ contribute little to the reconstructed image. The reconstructed toroidal component only shows up in low-degree (though non-axisymmetric) modes.

Since our τ Sco spectropolarimetry spans several rotation cycles, and since several phase ranges were observed more than once (phases ∼0.00, 0.47 and 0.85; see Table 1), we can directly investigate whether the magnetic field of τ Sco exhibits signs of variability on a timescale of about a year. We find that profiles obtained at very similar phases in different cycles (e.g., at cycles 2.02 and 10.01) agree to within the noise level.

We can also estimate how much latitudinal shear the magnetic topology of τ Sco experienced between 2004 Sep. and 2005 Sep., using the methods employed for cool stars by Petit et al. (2002) and Donati et al. (2003); we find no evidence for differential rotation at the surface of τ Sco, with
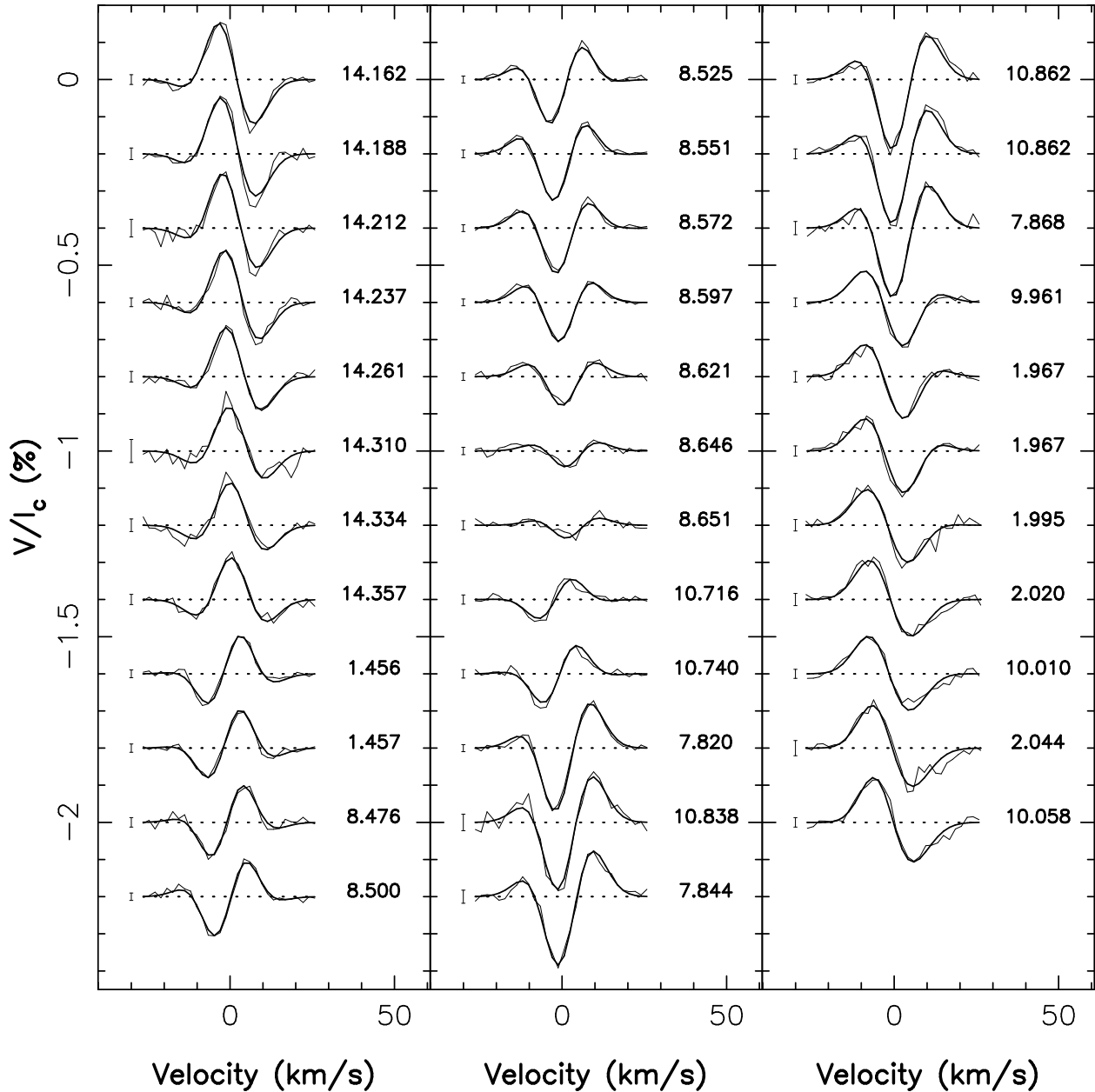
Figure 7. Maximum-entropy fit (thick lines) to the observed Zeeman signatures of τ Sco (thin lines). The rotational phase and cycle of each observation is written next to each profile. A 3σ error bar is also plotted left to each profile.

an upper limit of about 3 mrad d^{-1} (i.e., at least 20 times smaller than for the Sun). This is in agreement with our finding that the rotational modulation of UV lines, presumably related to the magnetic topology (Sec. 7.3.1), is stable over timescales of decades (Sec. 3.2).

We emphasize that only moderate surface spatial resolution can be obtained for τ Sco, as a result of its low rotation velocity; close bipolar groups, for example, could therefore easily remain undetected if present on scales smaller than the resolution element. However, given the dense phase coverage obtained throughout the whole rotation cycle, the large-scale magnetic field of τ Sco (up to orders with $\ell \simeq 6$), as well as its non-variability on a time scale of about 1.5 yr, is very well constrained by our observations.

6   ORIGIN OF THE FIELD

Using the magnetic map we derived for τ Sco, and thanks in particular to its unusual degree of complexity (by the standards of early-B and O-type stars), several questions can be addressed regarding the physics of massive stars. Our results both give us the opportunity to rediscuss the problem of the origin of magnetic fields in very hot stars, and also enable us to investigate the impact of complex fields on radiatively driven winds.

Although the classical picture was that magnetic fields of hot stars were presumably fossil remnants from the formation stage, the situation has changed considerably, with regular reports from both observers and theoreticians that massive stars may be able to generate dy-
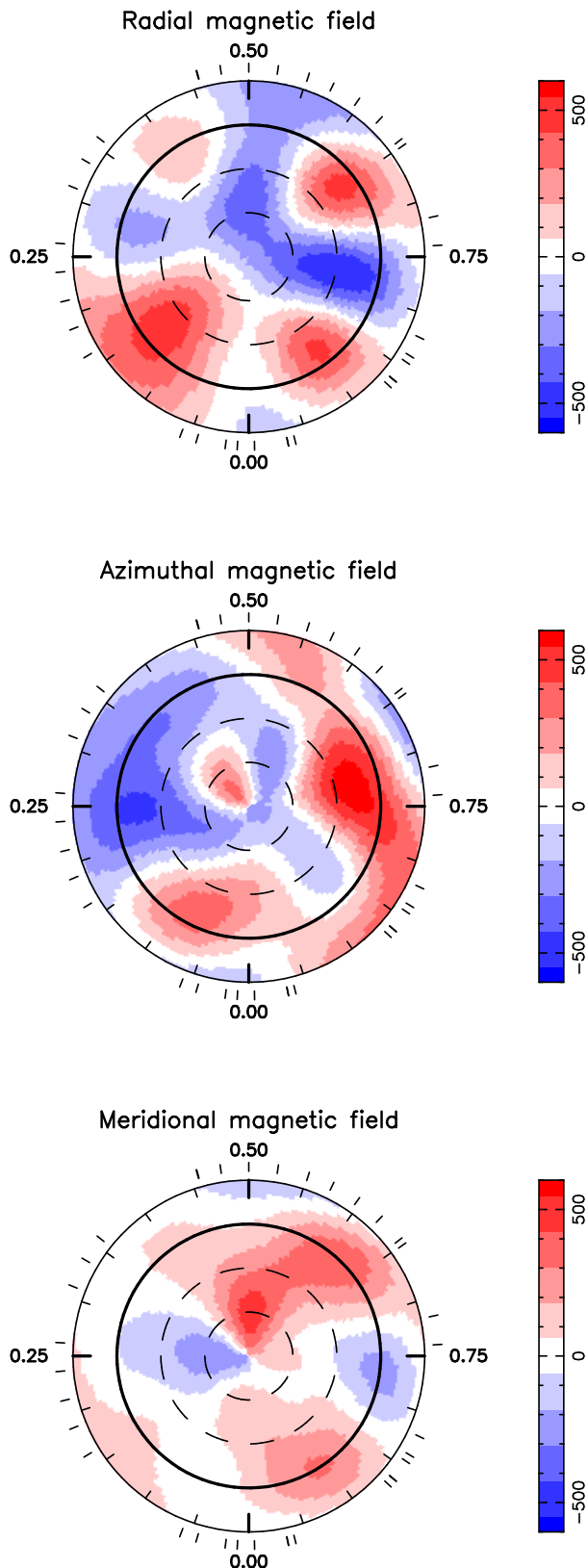
Radial magnetic field

Azimuthal magnetic field

Meridional magnetic field

Figure 8. Maximum-entropy reconstructions of the magnetic topology of τ Sco, assuming that the global field can be expressed as the sum of a potential field and a toroidal field. The three components of the field are displayed from top to bottom (flux values labelled in G). The top image (radial field component) is described through the set of complex coefficients $\alpha_{\ell,m}$ (see Sec. 5). The star is shown in flattened polar projection down to latitudes of $-30°$, with the equator depicted as a bold circle and parallels

namo processes, either deep inside their convective cores (Charbonneau & MacGregor 2001; MacDonald & Mullan 2004; Brun et al. 2005), within the greater part of their radiative envelope (Spruit 1999, 2002; MacDonald & Mullan 2004; Mullan & MacDonald 2005; Maeder & Meynet 2005; Braithwaite 2006), or in a subsurface layer (Tout & Pringle 1995; Lignières et al. 1996). In each case, different processes are invoked to explain the generation of magnetic fields. How do these proposals stand up in the particular case of τ Sco?

6.1 Dynamo processes?

Being intrinsically a very slow rotator (the second slowest rotator among massive stars after HD 191612; Donati et al. 2006), τ Sco does not seem to be an optimal candidate for triggering dynamo processes. Of course, one may argue that the rotation rate of the inner stellar regions may be far larger than that at the surface; evolutionary models tend, however, to indicate that the radial gradient in rotation rate is only moderate in massive stars, particularly in those hosting magnetic fields (Maeder & Meynet 2003, 2004, 2005).

Wherever they operate (whether in the convective core, the radiative envelope, or a subsurface layer), dynamo processes are all expected to strengthen with rotation rate and to vanish when rotation is slow; they should therefore be relatively weak in a star like τ Sco. In the particular case of the Spruit–Tayler dynamo processes (Spruit 1999, 2002), for example, field strengths only of order a few G are expected to appear at the surface of a star with a rotation rate as small as that of τ Sco (Mullan & MacDonald 2005), much lower than we have found. In the case of the core-dynamo hypothesis, MacDonald & Mullan (2004) demonstrate that surface magnetic fields need to originate in core fields that largely exceed the equipartition value, which is again highly unlikely in a slowly rotating star.

A second observation is that the magnetic features we reconstruct at the surface of τ Sco are present at essentially all latitudes. This is not compatible with the predictions of the Spruit–Tayler dynamo model with buoyancy included to allow magnetic flux rise up to the surface, which should produce magnetic regions concentrated at intermediate latitudes (Mullan & MacDonald 2005). Nor is it compatible with the core-dynamo theory, which predicts that flux tubes should mostly show up very close to the pole at the surface of the star (MacDonald & Mullan 2004).

Our observations further indicate that the reconstructed magnetic field is mostly poloidal, and includes no more than a moderate surface toroidal component. This is not compatible with dynamos operating in a shear layer below the surface or within the convective zone, which are expected to produce strong axisymmetric azimuthal fields (e.g., Braithwaite 2006) that should likely show up at photospheric level, and should even dominate the global magnetic map in the case of a sub-surface shear layer (as they do in stars with very shallow subsurface convective zones; e.g., Marsden et al. 2006). Moreover, we observe that the photosphere of τ Sco experiences negligible latitudinal shear (at least 20 times smaller than that of the Sun). Again, this is most probably inconsistent with a subsurface shear-layer dynamo, which is expected to generate azimuthal and radial gradients of angular velocity, at least within the shear layer itself.
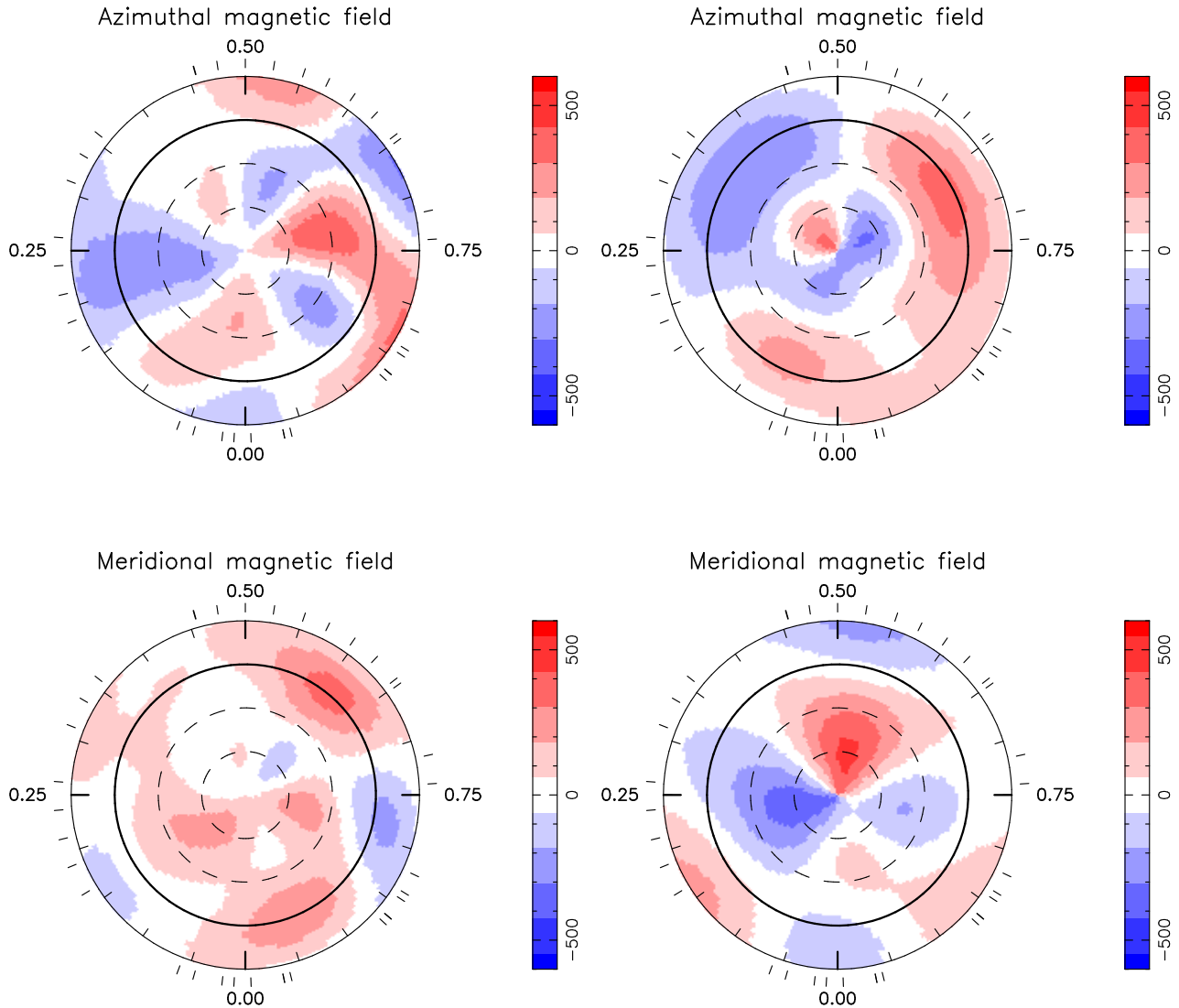
Figure 9. Azimuthal and meridional components of the reconstructed potential (left column) and toroidal (right column) field structures. Adding both together yields the azimuthal and meridional field components shown in Fig. 8. The image on the left hand side is described through the set of complex coefficients $\beta_{\ell,m}$ while that on the right hand side is obtained through the coefficients $\gamma_{\ell,m}$ (see Sec. 5).

An additional argument against dynamo processes is that they should essentially succeed (if conceptually valid) at producing magnetic fields in most hot stars and not only in a small fraction of them. The fact that magnetic fields are detected in a star like τ Sco, known for its peculiar spectroscopic morphology (e.g., through its abnormally strong UV P-Cygni lines and its unusually hard X-ray emission), after having been detected in other peculiar hot stars (like θ^1 Ori C, HD 191612 and β Cep), represents further evidence that magnetic fields (at least those of moderate to high intensity) are not a common feature of most hot stars, but rather a rare occurence. In this respect, the parallel between massive hot stars with intermediate-mass ones, for which only about 10% of them are magnetic, seems strengthened by our new result.

Finally, the magnetic configuration of τ Sco exhibits no

sign of variability evident on a timescale of a year or so.[8] Archival IUE data provide a further, albeit indirect, indication that the field topology is probably stable on timescales of decades. Although all dynamo models proposed for hot stars predict some kind of temporal variability, little information is available on the typical timescale on which the surface fields are expected to evolve. At least for models depending on differential rotation, we can expect the field configuration within the star to evolve on timescales shorter

---

[8] We note that two longitudinal-field estimates obtained for τ Sco by Landstreet (1982), -61 ± 30 G and -16 ± 23 G and on JDs 2,442,174.92 and 2,442,175.89 respectively, average to a longitudinal field of -33 ± 18 G at a phase 0.49 (cycle -169) according to eqn. 1. The longitudinal field we measure at this phase, -20 ± 3 G, is compatible with the estimate given by Landstreet (1982) to within the errors, and provides additional (though admittedly fairly weak) evidence that the magnetic field of τ Sco exhibits no intrinsic variability on timescales of decades.

Mode amplitude   Mode amplitude   Mode amplitude
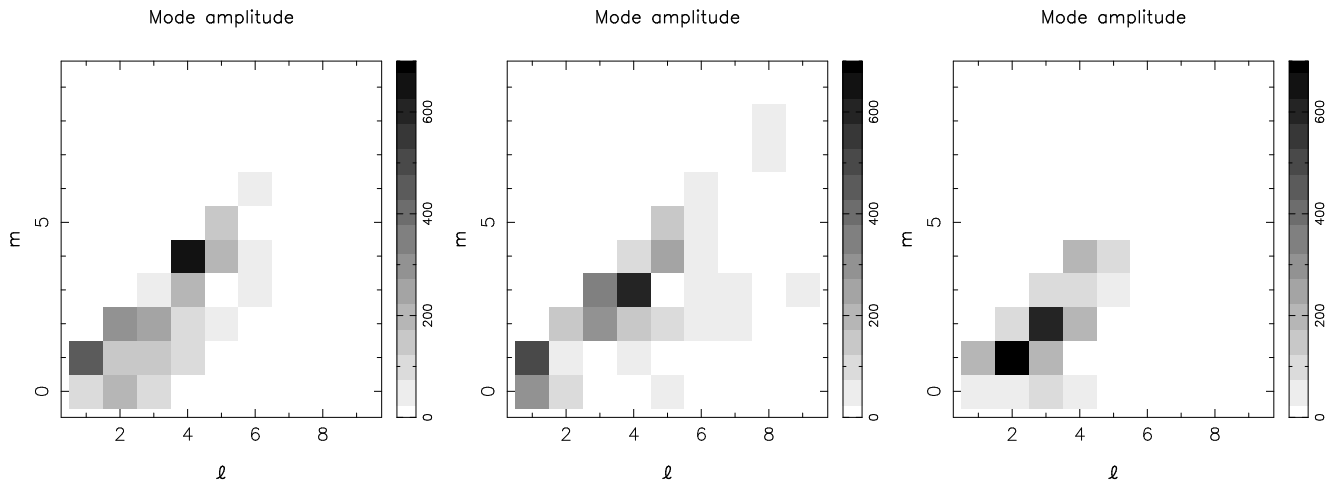

Figure 10. Modulus (in G) of the spherical-harmonic complex coefficients $\alpha_{\ell,m}$, $\beta_{\ell,m}$ and $\gamma_{\ell,m}$ (see Sec. 5) for the reconstructed magnetic-field topology of τ Sco, as a function of mode degree ℓ and order m. These sets of coefficients respectively correspond to the magnetic images shown in the top panel of Fig. 8 (radial field component), left panels of Fig. 9 (azimuthal and meridional component of potential field term) and right panels of Fig. 9 (azimuthal and meridional component of toroidal field term). Only modes with $\ell < 10$ are displayed here.

than a year, as buoyant flux tubes typically need timescales of order a year to travel to the surface in a star like τ Sco (provided the field in the flux tube is not too weak compared to the local equipartition value; MacDonald & Mullan 2004), again implying that the observed non-variability argues against the proposed dynamo models.

Recent numerical results by Braithwaite & Spruit (2004) and Braithwaite & Nordlund (2006) also indicate that magnetic fields in hot stars seem to reach a stable equilibrium (involving both potential and toroidal fields) but are not self-amplified by instability processes, unless the star features self-sustained differential rotation (Braithwaite 2006). Similar numerical results are obtained by Brun and collaborators (Zahn, personal communication). Our result indicates that τ Sco is likely not a differential rotator (as it would otherwise host strong axisymmetric toroidal fields like those seen on cool stars, Donati et al. 2003); it may therefore be fairly natural that no evidence for dynamo action is detected on τ Sco.

6.2 Fossil fields?

The next step is to compare our observations with predictions of the fossil-field theory. Since τ Sco is rather young (a few Myr; Sec. 4), the complexity of the field we detected is probably not a problem; while low-order terms (with longer decay times) are expected to dominate the fossil magnetic topologies of old stars, higher-order terms should still be present in stars as young as τ Sco. Moreover, very little differential rotation and variability (on a ∼yearly timescale) is expected to occur in stars hosting superequipartition fossil magnetic fields, in agreement with what we find.

Both toroidal and poloidal fields of comparable strength are expected to be present within the star, at least to ensure dynamical stability of the fossil field on long timescales (Moss 2001; Braithwaite & Spruit 2004; Braithwaite & Nordlund 2006). The prediction is that the expected toroidal field should be roughly axisymmetric (with respect to the poloidal magnetic axis) and concentrate

on the poloidal magnetic equator (Braithwaite & Spruit 2004; Braithwaite & Nordlund 2006). Although we indeed detect a small toroidal field at the surface of the star, its topology is not compatible with such predictions, which would require the toroidal field to coincide with the poloidal field equator (i.e. to show up mainly as a meridional field belt encircling the star, passing through both rotational poles and crossing the rotational equator at phases of about 0.3 and 0.8, see Sec. 7). Note however that theory expects the toroidal field to remain within the stellar interior; it may therefore be unsurprising not to detect it at photospheric level. We suggest that the toroidal field structure we detect at photospheric level rather results from the interaction of the stellar wind and the magnetic field (see Sec. 7).

Another attraction of the fossil-field theory is that there is no contradiction with the fact that the star is both magnetic and slowly rotating. Actually, we note that magnetic hot stars are, in average, even more slowly rotating than non-magnetic stars. One can, of course, wonder whether this is a real property of massive magnetic stars, or simply an observational bias (magnetic fields being easier to detect by spectropolarimetric methods in narrow-lined, slowly rotating stars); however, experiments clearly demonstrate that several rapidly rotating O stars (e.g., ζ Pup, ζ Ori) have surface magnetic fields with strengths not more than a few tens of G (Donati, in preparation). The youth of τ Sco excludes the possibility that slow rotation is a result of angular-momentum loss through a magnetic wind during the main-sequence phase;[9] thus the most probable option is that this situation is due to a process occuring during the formation stage. The idea proposed for magnetic, chemically-peculiar stars (also more slowly rotating in average than

---

[9] Following Donati et al. (2006), we evaluate the magnetic-braking timescale of τ Sco to be of order of 5 Gyr. As this timescale is some 3 orders of magnitude larger than the age of τ Sco, we can safely conclude that angular-momentum loss through the current magnetically confined wind is not responsible for the slow rotation.

non-magnetic stars of similar spectral type), invoking magnetic coupling with a putative accretion disc (Stępień 2000), is probably not applicable in the case of massive stars, which do not exist as stars during the formation stage and directly appear onto the main sequence. One possibility is that protostellar discs with intrinsically higher primordial magnetic fields are more successful at expelling angular momentum from the disc (e.g., through magnetic jets) than those with weak primordial fields, leading to magnetic hot stars rotating more slowly than non-magnetic counterparts of similar mass.

6.3   Conclusion

Taking all these arguments into consideration, we find that the magnetic topology we have reconstructed for τ Sco is more likely to be of fossil origin than to be generated by any of the various dynamo mechanisms proposed up to now in the literature. If this is confirmed, it would indicate that very hot magnetic stars probably represent a high-mass extension of the classical Ap/Bp phenomenon; the reason these massive magnetic stars do not mark themselves as chemically peculiar is probably related to their strong winds, which prevent photospheric element stratification building up. This scenario would also argue in favour of the proposition of Ferrario & Wickramasinghe (2005, 2006), who suggested that massive magnetic stars are the progenitors of highly magnetic neutron stars.

7   THE EXTENDED MAGNETOSPHERIC STRUCTURE

A second topic of interest is the impact of the magnetic field on the radiatively driven wind of τ Sco. In particular, τ Sco gives us the opportunity of investigating the confining effect of magnetic fields whose topology is more complex than those of other early B and O stars for which similar studies have been carried out (Donati et al. 2001, 2002; Gagné et al. 2005b,a).

In the now-standard picture, initially proposed by Babel & Montmerle (1997) and further investigated by Donati et al. (2001, 2002), ud-Doula & Owocki (2002), Townsend & Owocki (2005) and Gagné et al. (2005b,a), the magnetic field is assumed to be dipolar; the dense wind coming from each magnetic hemisphere is deflected by the field towards the magnetic equator, where it produces a strong shock, a very hot X-ray emitting post-shock region (reaching temperatures of 10^7 K), and a cool, dense disk in the magnetic equator, where the plasma accumulates before being ejected away from, or accreted back onto, the star (depending on the local radial velocity of the plasma when it reaches the disc, and on the effective gravity in the disc at this point).

For a more complex magnetic topology, the picture is expected to differ significantly. The extended magnetic structure should show a correspondingly greater degree of complexity, involving distinct regions of closed loops alternating with regions of open field lines, rather than two open-field polar cones and one closed-field magnetic torus, as in the dipole field case. Wind flows should freely escape the star along open field regions and should produce shocks and very

hot X-ray emitting plasma within each closed-field region, with cool, dense condensations forming at loop summits. The resulting magnetospheric structure should therefore begin to resemble that of the Sun, with hot coronal arcades confining cool, dense, prominence-like structures (the main difference being, of course, the heating mechanism itself).

7.1   The magnetic-confinement parameter

First, to evaluate to what distance from the star the wind of τ Sco is magnetically confined, it is useful to consider the wind magnetic-confinement parameter η, defined by ud-Doula & Owocki (2002) to characterize the ratio between the magnetic-field energy density and the kinetic energy density of the wind:

$$\eta = B^2 R_\star{}^2 / \dot{M} v_\infty, \tag{9}$$

where B is the typical magnetic-field strength, $\dot{M}$ is the average mass-loss rate, and v_∞ is the terminal wind velocity. Our study demonstrates that B is in average $\simeq 300$ G over the surface of τ Sco. However, there is a substantial dispersion in published estimates of $\dot{M}$, with recent determinations ranging 0.2–6×10^{-8} $M_\odot\,\mathrm{yr}^{-1}$ (e.g., Mokiem et al. 2005; Repolust et al. 2005); we adopt a value of 2×10^{-8} $M_\odot\,\mathrm{yr}^{-1}$ as a reasonable average of modern observational determinations. Observations also suggest a terminal velocity of about $2,000$ $\mathrm{km\,s}^{-1}$ (e.g., Abbott 1978), but line-driven wind theories predict a significantly higher value (up to $3,800$ $\mathrm{km\,s}^{-1}$, Pauldrach 1987; note, however, that the stellar parameters used for these theoretical studies, and in particular the mass, temperature, luminosity and radius of τ Sco, are all significantly overestimated compared to modern values). We adopt $v_\infty = 2,000$ $\mathrm{km\,s}^{-1}$ (Mokiem et al. 2005).

With these values, we find that the wind confinement parameter is about 40, and thus that the Alfven radius, above which all closed magnetic loops open under the wind ram pressure, is of order of 2 $R_\star$. This is in good agreement with the findings of Cohen et al. (2003), based on Chandra observations (and in particular on Si XIII and Mg XI line ratios), that the X-ray emitting plasma is located at average distances of about 1 $R_\star$ above the surface[10].

Arguably, this agreement may be partly coincidental, given the large uncertainty on $\dot{M}$; if it were 10 times smaller than the value we adopted, with all other parameters held fixed, η would reach a value of 400. The magnetosphere would then be confined out to significantly larger distances (typically of order $4R_\star$); we should then detect hard X-ray emission from loops extending several $R_\star$ above the stellar surface, which is apparently not the case. If $\dot{M}$ were larger than 6×10^{-8} $M_\odot\,\mathrm{yr}^{-1}$, then η would be smaller than 10, and no stable magnetic loops extending further than 0.3 $R_\star$ above the surface would survive the wind pressure (e.g., ud-Doula & Owocki 2002), again in contradiction with X-ray observations. We therefore conclude that, if this model is correct, X-ray observations constrain η to values ranging

---

[10] A recent re-analysis of the Chandra τ Sco spectra using updated atomic data (e.g., Gagné et al. 2005a) indicates that all line ratios from He-like ions (including both Si XIII and Mg XI) are consistent with the X-ray emitting plasma being concentrated at a distance of about 1 $R_\star$ above the photosphere (Cohen 2006, personal communication).
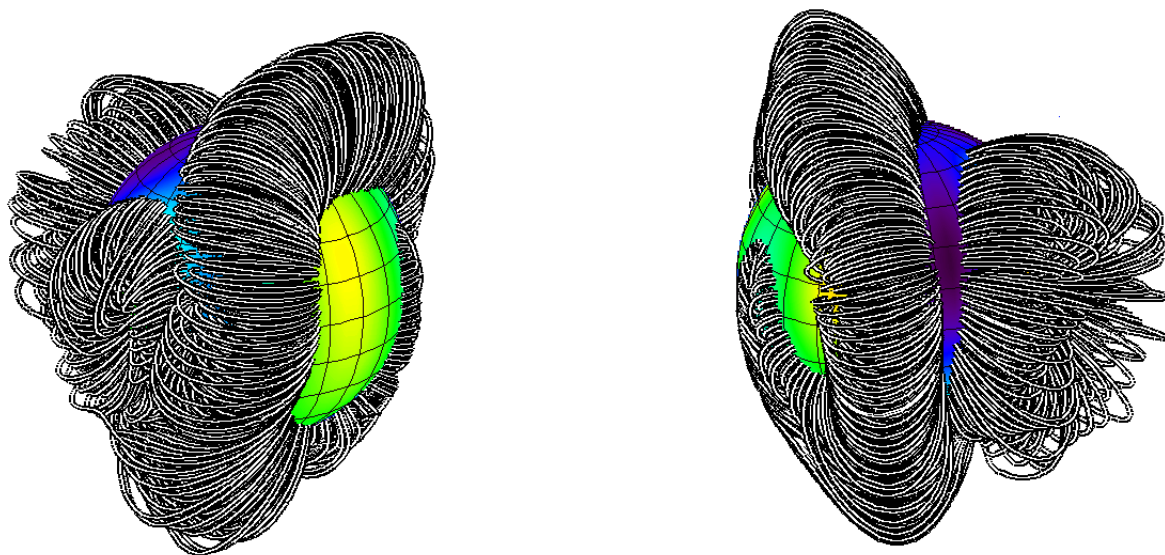
Figure 11. Closed magnetic-field lines of the extended magnetic configuration of τ Sco, extrapolated from the photospheric map of Fig. 8. The star is shown at phases 0.25 (left) and 0.83 (right). Note the warp of the magnetic equator and the additional network closed loops around phase 0.65 (mostly visible on the right side of the right panel).
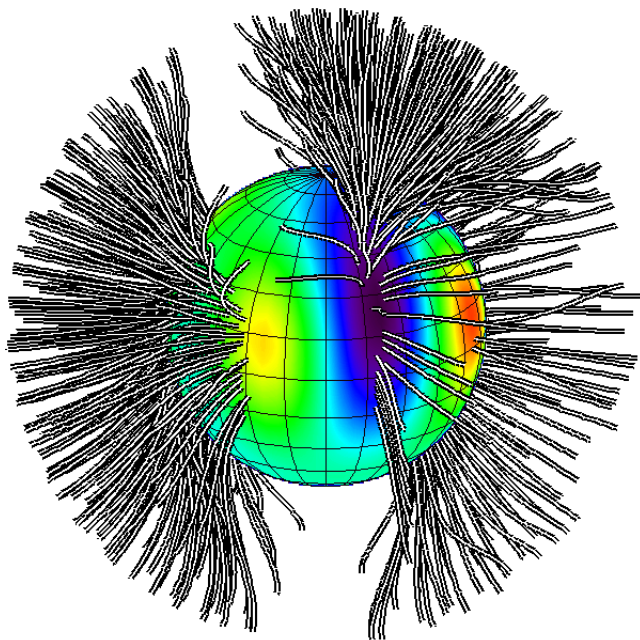

Figure 12. Open field lines of the extrapolated extended magnetic configuration. The star is shown at phase 0.83 only.

typically within 20 to 100, and hence the mass-loss rate to values of 1–4×10^{-8} M$_\odot$ yr^{-1}.

7.2 Magnetic-field extrapolation

Using the field-extrapolation technique of Jardine et al. (1999), with a spherical source function set to $2\,R_\star$ (to mimic the mainly radial orientation of the field lines at distances larger than $2\,R_\star$), we can draw inferences on the large-scale magnetospheric structure of τ Sco, presented in Figs. 11 (closed field lines) and 12 (open field lines). We find that the extended field structure is significantly more complex than a global dipole, even though it still features a torus of closed magnetic loops encircling the star (with an axis of symmetry roughly tilted at $\simeq$90deg to the rotation axis; Fig. 11) and two main cones of open field lines on opposite sides of the star (see Fig. 12). In particular, the magnetospheric equator is significantly warped, and additional networks of closed loops are present at low latitudes (e.g., one around phase 0.65, left panel of Fig. 11, in conjunction with the equatorial region of positive radial field reconstructed at this phase, another one around phase 0.4). Most closed loops typically extend to a distance of up to $2\,R_\star$, in reasonable agreement with constraints derived from Chandra data.

Note that these small networks of closed loops (at phases 0.40 and 0.65) both coincide with local maxima of the reconstructed toroidal field component (see top right panel of Fig. 9); from this apparent spatial correlation, we speculate that the toroidal field component we detect may be produced through an interaction of the stellar wind and the magnetic field right at the photospheric level. We also note that these loops roughly coincide with the rotation phase at which the unpolarised line profile of τ Sco is slightly narrower than average; again, this may reflect the particular wind configuration that results from this specific field configuration at the stellar surface. MHD simulations are of course needed to confirm whether this idea is realistic or not.

7.3 Observational implications

7.3.1 Optical and UV diagnostics

This model implies that excess absorption in UV lines should occur when the magnetospheric equatorial plane crosses the line of sight, as in all similar hot magnetic stars (e.g., Donati et al. 2001, 2002, 2006; Neiner et al. 2003), i.e., at phases 0.3 and 0.8 – in excellent agreement with observations (see Fig. 5). In particular, the fact that the two UV absorption events we detect are largely similar in shape, and separated by 0.5 rotation cycles, provides independent confirmation that either the angle i of the rotation axis to the line-of-sight (which we found to be $\simeq 70°$), or the global tilt of the large-scale magnetic structure to the rotation axis (for which we derived an estimate of $\sim 90°$), or both, is/are large. As mentioned previously, the relative phasing between our new spectropolarimetric data and the old archival IUE spectra is accurate enough (of order 1%; Sec. 3.2) to ensure that this match is not a coincidence; it thus provides a strong argument in favour of the present model.

Photometric measurements secured by Hipparcos indicate a constant flux level (to within 10 mmag), showing that the column density of the wind material trapped within the magnetospheric equator of τ Sco is not high enough to produce detectable light variations through scattering, even when the disc is seen edge-on. This situation is similar to that found for β Cep and θ Ori C (for which no photometric variations are detected; Donati et al. 2001, 2002), but differs from HD 191612 and σ Ori E (for which eclipses of the continuum radiation by the magnetospheric plasma are observed, at levels of 0.04 and 0.15 mag, respectively; Walborn et al. 2004; Townsend & Owocki 2005; Donati et al. 2006).

In our data, we detect no rotational modulation of the Hα flux from τ Sco, mimicking what is observed in β Cep (which shows only long-term Hα variations), but very different to θ Ori C, σ Ori E and HD 191612 (all of which exhibit strong Hα modulation; Stahl et al. 1996; Townsend & Owocki 2005; Walborn et al. 2003). More modelling is required to check whether these observations are compatible with the basic picture presented here; this is postponed for a future study.

7.3.2 X-ray diagnostics

The wind pressure at the base of the the postshock region is given by

$$p_{\rm w} = \epsilon \, \dot{M} v_\infty / 4\pi R_\star{}^2, \tag{10}$$

to first order, where $\epsilon = 1/x^2 - 1/x^3$ and x is the radial distance from the centre of the star at which the equilibrium location of the shock front settles (in units of $R_\star$). For a range of reasonable values of x ($\sim$1.2–1.7), ϵ remains roughly constant ($\sim$0.10–0.15), implying a wind pressure of about 20–30 g cm^{-1} s^{-2}. This corresponds to a number density of protons and electrons of about 10^{10} cm^{-3} for a postshock temperature of order 10^7 K within the loop. Again, this is in good agreement with the upper limits on the electron density derived by Cohen et al. (2003) from Chandra data. By assuming that the closed 'corona' (the equatorial magnetospheric torus and the small additional networks of closed loops) is filled with such a plasma, and using the

simple coronal-structure model of Jardine et al. (2002), we find that the resulting emission measure is of order of a few 10^{54} cm^{-3}, in reasonable agreement with actual measurements from X-ray spectra (Wojdowski & Schulz 2005). This result essentially indicates that, in the model we have devised, the observed X-ray emission can be mostly attributed to the magnetosphere (and that the model is therefore broadly consistent with X-ray observations).

If our speculation is correct, it implies that the X-ray emission of τ Sco should be modulated on a timescale equal to the rotation period (i.e., 41 d), as a result of the magnetosphere being partially eclipsed by the stellar disc in appropriate viewing configurations. We estimate the expected fractional modulation to be about 40%, i.e., comparable to that of θ Ori C (Gagné et al. 2005a,b), but should feature two main eclipse episodes each rotation cycle, centred on phases $\sim$0.3 and 0.8 (concomitant with the UV line-absorption events witnessed in IUE spectra); this should be easily detectable given adequate temporal sampling.

Checking such predictions should provide a strong test of our model. If the observed X-ray rotational modulation is much weaker than expected, it could imply that most of the magnetospheric emission is produced in small-scale loops evenly spread over the stellar surface; this would argue for additional, high-order components of the magnetic topology that we are not able to detect in this study (as a result of the limited spatial resolution provided by Doppler imaging for stars rotating as slowly as τ Sco).

At this stage, a more accurate model is obviously necessary to confirm the conclusions of the present paper, and to develop in more detail how well the X-ray spectrum of τ Sco can be reproduced once the magnetospheric structure, including the wind-induced expansion of magnetic loops, is consistently taken into account. Such a sophisticated model should also aim to reproducing the observed modulation of UV spectra and the upper limits on the photometric and Hα flux variability (e.g., as done for σ Ori E by Townsend et al. 2005).

8 CONCLUSION

We have reported the detection of a magnetic field on the massive B0.2 V star τ Sco, using data obtained mostly with ESPaDOnS, the new high-resolution stellar spectropolarimeter recently installed at CFHT. From the Zeeman signatures and their temporal variability, we were able to identify the rotation period of τ Sco and to reconstruct the large-scale topology of its photospheric field. Archival IUE spectra confirm that the rotational modulation is stable on timescales of decades, with $P_{\rm rot} \simeq 41.03$ d.

We find that the surface magnetic topology is unusually complex (judged by the small sample of massive-star results) and is mostly potential. It also includes a moderate toroidal component; in particular, the strength of this toroidal component (relative to that of the poloidal component) is much lower than that found in partly-convective cool stars hosting dynamo-generated magnetic fields. No temporal variability of the magnetic structure is detected over the 1.5-yr period of our observations; we thus conclude that any surface differential rotation of τ Sco is at least 20 times weaker than that of the Sun.

We determine that the large-scale magnetospheric structure of τ Sco is significantly more complex than a global dipole; it features in particular a significantly warped torus of closed magnetic loops encircling the star, tilted at about $90°$ to the rotation axis, as well as additional (smaller) networks of closed field lines. The extended magnetic topology we derive from extrapolations of the photospheric magnetic maps is apparently compatible with the published X-ray luminosity and spectral characteristics of τ Sco. Our model is also compatible with the observed modulation of UV spectral lines. We predict that τ Sco should exhibit a clear rotational modulation of its X-ray emission.

From these results, we conclude that its magnetic field is most probably a fossil remnant from the formation stage. We cannot yet completely rule out the possiblity that the field is produced through one of the recently-elaborated dynamo processes that may operate in the radiative zones of hot stars, but our findings already indicate that this option is rather unlikely.

ACKNOWLEDGEMENTS

REFERENCES

Abbott D., 1978, ApJ, 225, 893
Aitken D., Hough J., 2001, PASP, 113, 1300
Babel J., Montmerle T., 1997, ApJ, 485, L29
Boggess A., Carr F., Evans D., Fischel D., Coleman C., Snijders M., Wilson R., 1978, Nature, 275, 372
Borra E., Landstreet J., 1980, ApJS, 42, 421
Braithwaite J., 2006, A&A, 449, 451
Braithwaite J., Nordlund A., 2006, A&A, in press
Braithwaite J., Spruit H., 2004, Nature, 431, 819
Brown S., Donati J.-F., Rees D., Semel M., 1991, A&A, 250, 463
Brun A., Browning M., Toomre J., 2005, ApJ, 629, 461
Charbonneau P., MacGregor K., 2001, ApJ, 559, 1094
Cohen D., Cassinelli J., Waldron W., 1997, ApJ, 488, 397
Cohen D., de Messières G., MacFarlane J., Miller N., Cassinelli J., Owocki S., Liedahl D., 2003, ApJ, 586, 495
de Zeeuw P., Hoogerwerf R., de Bruijne J., Brown A., Blaauw A., 1999, AJ, 117, 354
Donati J.-F., 2001, in Boffin H., Steeghs D., Cuypers J., eds, Astrotomography: Indirect Imaging Methods in Observational Astronomy Vol. 573 of Lecture Notes in Physics, Imaging the Magnetic Topologies of Cool Active Stars. Springer, Berlin, p. 207
Donati J.-F., Babel J., Harries T., Howarth I., Petit P., Semel M., 2002, MNRAS, 333, 55
Donati J.-F., Brown S., 1997, A&A, 326, 1135
Donati J.-F., Cameron A., Semel M., Hussain G., Petit P., Carter B., Marsden S., Mengel M., Lopez Ariste A., Jeffers S., Rees D., 2003, MNRAS, 345, 1145
Donati J.-F., Catala C., Wade G., Gallou G., Delaigue G., Rabou P., 1999, A&AS, 134, 149
Donati J.-F., Howarth I. D., Bouret J.-C., Petit P., Catala C., Landstreet J., 2006, MNRAS, 365, L6
Donati J.-F., Semel M., Carter B., Rees D., Collier Cameron A., 1997, MNRAS, 291, 658
Donati J.-F., Wade G., Babel J., Henrichs H., de Jong J., Harries T., 2001, MNRAS, 326, 1256
Ferrario L., Wickramasinghe D., 2005, MNRAS, 356, 615
Ferrario L., Wickramasinghe D., 2006, MNRAS, 367, 1323
Gagné M., Oksala M., Cohen D., Tonnesen S., ud-Doula A., Owocki S., Townsend R., MacFarlane J., 2005a, ApJ, 634, 712
Gagné M., Oksala M., Cohen D., Tonnesen S., ud-Doula A., Owocki S., Townsend R., MacFarlane J., 2005b, ApJ, 628, 986
Howarth I., Siebert K., Hussain G., Prinja R., 1997, MNRAS, 284, 265
Howk J., Cassinelli J., Bjorkman J., Lamers H., 2000, ApJ, 534, 348
Hussain G., Jardine M., Cameron A., 2001, MNRAS, 322, 681
Jardine M., Barnes J., Donati J.-F., Cameron A., 1999, MNRAS, 305, L35
Jardine M., Wood K., Cameron A., Donati J.-F., Mackay D., 2002, MNRAS, 336, 1364
Kilian J., 1992, A&A, 262, 171
Kurucz R., 1993, CDROM # 13 (ATLAS9 atmospheric models) and # 18 (ATLAS9 and SYNTHE routines, spectral line database). Smithsonian Astrophysical Observatory, Washington D.C.
Landstreet J., 1982, ApJ, 258, 639
Lignières F., Catala C., Mangeney A., 1996, A&A, 314, 465
MacDonald J., Mullan D., 2004, MNRAS, 348, 702
Maeder A., Meynet G., 2003, A&A, 411, 543
Maeder A., Meynet G., 2004, A&A, 422, 225
Maeder A., Meynet G., 2005, A&A, 440, 1041
Marsden S., Donati J.-F., Semel M., Petit P., Carter B., 2006, MNRAS, (submitted)
Mokiem M., de Koter A., Puls J., Herrero A., Najarro F., Villamariz M., 2005, A&A, 441, 711
Moss D., 1982, MNRAS, 201, 385
Moss D., 2001, in Mathys G., Solanki S., Wickramasinghe D., eds, Magnetic Fields Across the Hertzsprung-Russell Diagram Vol. 248 of ASP Conf. Proc., Magnetic Fields in the Ap and Bp Stars: a Theoretical Overview. San Francisco, p. 305
Moss D., 2003, in Arnaud J., Meunier S., eds, Magnetism and Activity of the Sun and Stars Vol. 9 of EAS, Fossil Stellar Magnetic Fields: Do They Exist, Does It Matter. EDP Sciences, Les Ulis, France, p. 21
Mullan D., MacDonald J., 2005, MNRAS, 356, 1139
Neiner C., Geers V., Henrichs H., Floquet M., Frémat Y., Hubert A., Preuss O., Wiersema K., 2003, A&A, 406, 1019
Nichols J., Linsky J., 1996, AJ, 111, 517
Pauldrach A., 1987, A&A, 164, 86
Petit P., Donati J.-F., Cameron A., 2002, MNRAS, 334, 374
Repolust T., Puls J., Hanson M., Kudritzki R.-P., Mokiem M., 2005, A&A, 440, 261
Roberts D., Lehar J., Dreher J., 1987, AJ, 93, 968
Robinson R., Smith M., Henry G., 2002, ApJ, 575, 435

Semel M., 2003, A&A, 401, 1

Simon-Diaz S., Herrero A., Esteban C., Najarro F., 2006, A&A, 448, 351

Smith M., Cohen D., Gu M., Robinson R., Evans N., Schran P., 2004, ApJ, 600, 972

Smith M., Karp A., 1978, ApJ, 219, 522

Spruit H., 1999, A&A, 349, 189

Spruit H., 2002, A&A, 381, 923

Stahl O., Kaufer A., Rivinius T., Szeifert T., Wolf B., Gaeng T., Gummersbach C. A., Jankovics I., Kovacs J., Mandel H., Pakull M. W., Peitz J., 1996, A&A, 312, 539

Stępień K., 2000, A&A, 353, 227

Stickland D., Lloyd C., 1995, Obs, 115, 90

Thompson I., Landstreet J., 1985, ApJ, 289, L9

Tout C., Pringle J., 1995, MNRAS, 272, 528

Townsend R., Owocki S., 2005, MNRAS, 357, 251

Townsend R., Owocki S., Groote D., 2005, ApJ, 630, L81

ud-Doula A., Owocki S., 2002, ApJ, 576, 413

Wade G., Aurière M., Bagnulo S., Donati J.-F., Johnson N., Landstreet J., Lignières F., Marsden S., Monin D., Mouillet D., Paletou F., Petit P., Toqué N., Alecian E., Folsom C., 2006, A&A, in press

Wade G., Drouin D., Bagnulo S., Landstreet J., Mason E., Sylvester J., Alecian E., Böhm T., Bouret J.-C., Catala C., Donati J.-F., 2005, A&A, 442, L31

Walborn N., Howarth I., Herrero A., Lennon D., 2003, ApJ, 588, 1025

Walborn N., Howarth I. D., Rauw G., Lennon D., Bond H., Negueruela I., Nazé Y., Corcoran M., Herrero A., Pellerin A., 2004, ApJ, 617, L61

Walborn N. R., Panek R. J., 1984, ApJ, 286, 718

Wojdowski P., Schulz N., 2005, ApJ, 627, 953